On Technical Issues in the Analysis of Nonlinear Ship Motion and Structural Loads in Waves by a Time-Domain Rankine Panel Method

Kyong-Hwan Kim, Yonghwan Kim

Seoul National University

The present study introduces the analysis of nonlinear ship motion responses and structural loads in regular and irregular waves. Analysis of motion responses and corresponding structural loads is an essential part of ship design. Due to recent trend of building very large ships, the nonlinear analysis becomes important. The analysis of nonlinear ship motions and structural loads in time domain is not new in ship hydrodynamics. King( ), Lin and Yue(1990), and Nakos and Sclavounos(1993) introduced pioneering works in this study, and particularly the effort of the latter two gave births of LAMP and SWAN. Although strip-based or response-function-based nonlinear methods are available, their works are deserve to be considered as the mot significant so far. Recently we developed a time-domain Rankine panel method called WISH (computer program for Wave-Induced loads and SHip motion) under the support of six companies including Daewoo, Hyundai, Hanjin, Samgsung, STX, and Korean Register. In this abstract, several critical technical issues and findings observed in this development are described with examples.

Analysis of Nonlinear Ship Motion & Structural Loads in Time Domain: Development of WISH

There are a few different methods to consider nonlinearity involved in ship motions. To make a long story short, the nonlinear effects can be categorized into two distinct nonlinearities: nonlinearity due to hull geometry and free-surface nonlinearity. In particular case of slender ships, it is generally assumed that the former takes a dominant role. Based on this assumption, the numerical method combining linear disturbed component with nonlinear Froude-Krylov and restoring components has been applied, e.g. SWAN2 and LAMP2. The same method is considered in the present study. Then the equation of motion can be written as follows:

$$[M]\{\ddot{\xi}_i\} = \{F_{Res.}\}_{Nonlinear} + \{F_{F.K.}\}_{Nonlinear} + \{F_{H.D.}\}_{Linear} \quad (1)$$

where $[M]$ and $\{\ddot{\xi}_i\}$ are mass matrix and acceleration of ship motion. $\{F_{Res.}\}$, $\{F_{F.K.}\}$, and $\{F_{H.D.}\}$ are restoring, Froude-Krylov and disturbed hydrodynamic forces. $\{F_{H.D.}\}$ can be obtained by solving the boundary value problem of the followings:

$$\frac{\partial \zeta_d}{\partial t} - (\underline{U} - \nabla\Phi)\cdot\nabla\zeta_d = $$
$$\frac{\partial^2 \Phi}{\partial z^2}\zeta_d + \frac{\partial \phi_d}{\partial z} + (\underline{U} - \nabla\Phi)\cdot\nabla\zeta_I \quad \text{on z=0} \quad (2)$$

$$\frac{\partial \phi_d}{\partial t} - (\underline{U} - \nabla\Phi)\cdot\nabla\phi_d = -\frac{\partial \Phi}{\partial t} - g\zeta_d + $$
$$\left[\underline{U}\cdot\nabla\Phi - \frac{1}{2}\nabla\Phi\cdot\nabla\Phi\right] + (\underline{U} - \nabla\Phi)\cdot\nabla\phi_I \quad \text{on z=0} \quad (3)$$

$$\frac{\partial \phi_d}{\partial n} = \sum_{j=1}^{6}\left(\frac{\partial \xi_j}{\partial t}n_j + \xi_j m_j\right) - \frac{\partial \phi_I}{\partial n} \quad \text{on mean body surface}$$
$$(4)$$

Φ, ϕ_I and ϕ_d are the double-body potential with steady speed, incident wave potential and disturbed wave potential, respectively. ζ is wave elevation, and subscript I and d indicate the incident and disturbed components.

To solve the prescribed boundary value problem, we can apply Green's second identity by discretizing

boundary surface. Particularly, in the present study, physical variables, i.e. velocity potential, wave elevation, normal flux along fluid boundary, are approximate using B-spline basis function.

$$\phi_d(\underline{x},t) = \sum_j (\phi_d)_j(t) B_j(\underline{x}), \ \zeta_d(\underline{x},t) = \sum_j (\zeta_d)_j(t) B_j(\underline{x}),$$

$$\frac{\partial \phi_d}{\partial n}(\underline{x},t) = \sum_j \left(\frac{\partial \phi_d}{\partial n}\right)_j (t) B_j(\underline{x}) \tag{5}$$

where $B_j(\underline{x})$ is basis function, and $(\phi_d)_j(t)$, $(\zeta_d)_j(t)$ and $(\partial \phi_d / \partial n)_j(t)$ are potential coefficient, wave elevation coefficient and coefficient of normal flux at the j-th discretized boundary segment, i.e. panel. By substituting Eq.(5) into Eqs.(2~4) and Green's second identity, we can assemble a matrix equation with unknown coefficients. By solving the matrix equation, the normal flux on free surface and the velocity potential on body surface can be obtained. Then wave elevation and potential on free surface are obtained by the time integration of Eqs.(2) and (3).

The nonlinear Froude-Krylov force and nonlinear restoring force can be computed using the followings:

$$(F_{Res.})_{nonlinear} = (F_{static})_{exact} - (F_{static})_{mean}$$
$$= \int_{S_B} \rho g(-z_e)\cdot n_j dS - \int_{\bar{S}_B} \rho g(-z_m)\cdot n_j dS \tag{6}$$

$$(F_{F.K.})_{nonlinear} = -\rho \iint_{S_B} \left[\left\{ \left(\frac{\partial}{\partial t} - \underline{U}\cdot\nabla\right)\phi_I \right\} \cdot n_j \right.$$
$$\left. + \left\{ \nabla\Phi\cdot\nabla\phi_I \right\} \cdot n_j + \left\{ \frac{1}{2}\nabla\phi_I\cdot\nabla\phi_I \right\} \cdot n_j \right] dS \tag{7}$$

where $S_B, \bar{S}_B$ are the instantaneous wetted surface by incident waves and body motion.

Technical Issues

<u>Directions for motion and structural loads</u>

Fig.1 shows the surge motion RAOs of S175 hull for different wave amplitudes at head sea and Fn=0.25, particularly comparing between SWAN and WISH. For consistency, nonlinear solution should recover linear solution when wave amplitude is very small. The two programs provide very different RAOs, and the consistency can be found only in WISH results. To find the source of this discrepancy, we carried out a systematic computation, and our finding is summarized in Table 1.
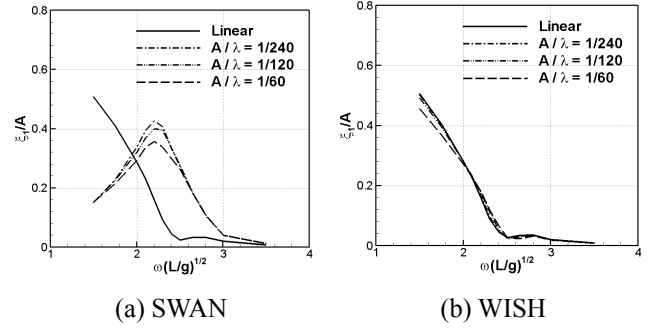

(a) SWAN   (b) WISH

Fig.1 Surge motion RAOs of S175 hull for different wave steepness: Fn=0.25, β=180 deg

Fig.2 Combination of directions for the equation of motion and the nonlinear loads

SWAN adopts the method of Case 1, while WISH applies Case 3. It should be noted that structural property for load computation is defined generally at ship sections along the ship length. Then, when the ship is under nonlinear motion, the direction to define the equation of motion can be instantaneously inconsistent with that for ship sections. This inconsistency can result in unbalanced force balance at the end of ship. What we found is that Case 3 provides the results consistent with linear solution for small wave amplitude with well-balanced structural loads.

Transom Condition

Categorizing three different types of stern flow is typical. The flow types are dependent on Froude number with respect to transom draft. According to Mantzaris(1998), implementing the following conditions provides good results for the transom flow when the Froude number is greater than 4.0:

$$\zeta_T = z_T, \quad \frac{\partial \zeta_T}{\partial x} = \frac{\partial z_T}{\partial x}, \quad \frac{\partial \zeta_T}{\partial y} = \frac{\partial z_T}{\partial y} \tag{8}$$

Numerical test are carried out with and without the stern-flow condition Eq.(8), and the motion responses of different ships are observed. Fig.3 shows two sample ships for the test: 5415 hull and a very large commercial ship with twin skegs. The former has a deep transom, while the latter has a shallow transom. Fig.4 and 5 show the difference of wave profiles with and without the implementation of Eq.(8) for the two ships. According to our experience, as these figures show, the motion responses are affected by the application of the transom condition for ships with deep transom running in high speed. However, in the speed range of most commercial ships with shallow transom, imposing the transom condition doesn't affect much the motion responses.
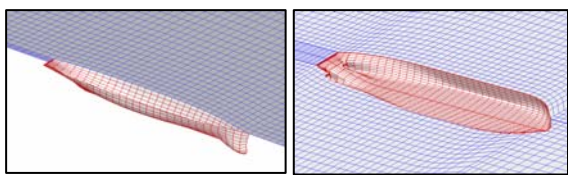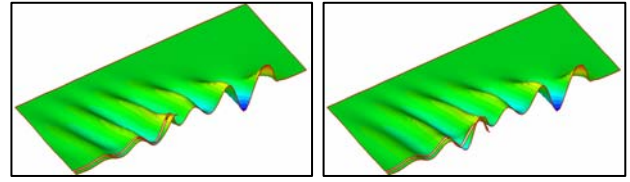

(a) 5415   (b) very large containership

Fig.3 Two ship models for testing transom condition
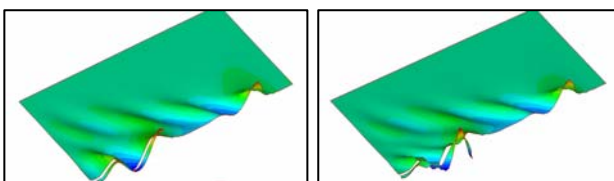
(a) Without   (b) Without

Fig.4 Comparison of wave profiles around 5415: with and without transom condition


(a) Without   (b) Without

Fig.5 Comparison of wave profiles around the very large containership: with and without transom condition

Grid Type

Two types of computation domain and mesh distributions are popular in the application of panel method for the ship motion analysis: rectangular and oval (circular) domains and mesh distributions. It is observed that generally oval domain and mesh distribution provides smoother and more reasonable solutions for diffraction and radiation problems. Since disturbed waves due to the existence and motion of a body propagate in radial direction eventually, the oval grid type seems to have generally better prediction of radiating waves.
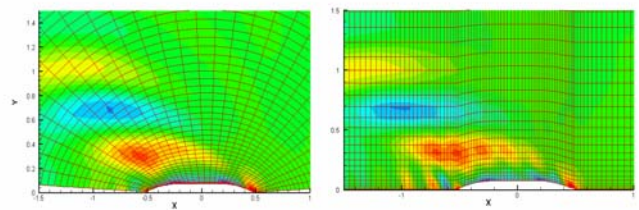
(a) Oval grid   (b) Rectangular grid

Fig.6 Effects of grid type on wave contours around Series 60 (C_b=0.7) under forced heave motions

Such observation is clear in Fig.6 in which compares wave contours around a Series 60 hull under forced heave motion with forward speed. On the other hand, when wave-resistance problem becomes more important, selecting rectangular grids may be a right choice.

Soft Spring or Course-Keeping

In time-domain approaches, surge, sway, and yaw motions diverge as time marches if there is no external

restoring force and/or moment. To make a problem more realistic, adoption of a course-keeping mechanism is desirable. However, in recent studies, application of soft spring is popular because of its simplicity, acceptable accuracy, and difficulties in controlling the gains of course-keeping algorithms. In this study, artificial springs are added in the equation of motion, which should not affect the motions of our interests and controls effectively the restoring, and their strengths are determined in order to have their natural frequency as follows:

$$T_i = 2\pi \sqrt{\frac{m_{ii} + m_{ii}(\infty)}{c_{ii}}} \ , \ c_{ii} = (m_{ii} + m_{ii}(\infty)) \times \left(\frac{2\pi}{T_i}\right)^2 \quad (9)$$

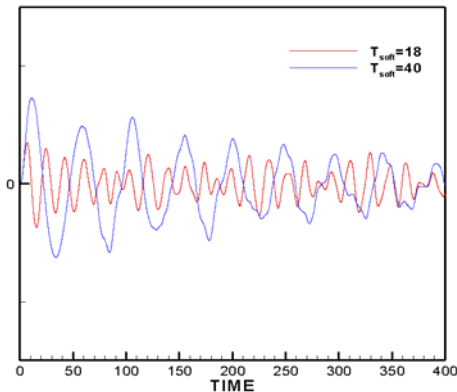where $m_{ii}(\infty)$ is infinite-frequency added mass, and $i=1,2,6$.

Fig.7 Surge signals with two soft spring coefficients: S175 hull, 120-deg heading, F_n=0.275

In our test, it is found that proper values of T_i, i.e. spring strength are sensitive to many parameters, including the ship speed, vessel type, location of spring, and so on. The detailed explanation is not described here. Fig.7 shows the surge signals with two different spring coefficients for S175 hull at F_n=0.275 in 120-deg heading, showing very significant difference.

Correction of Steady Component

It is found that structural loads are affected by steady component. Some existing studies have not considered

intentionally in the computation of wave excitation and structural loads. Fig.8 shows the longitudinal distribution if nonlinear sagging(+) and hogging(-) moments along S175 hull in irregular waves. There is non-ignorable difference of the loads between the cases with and without steady component.
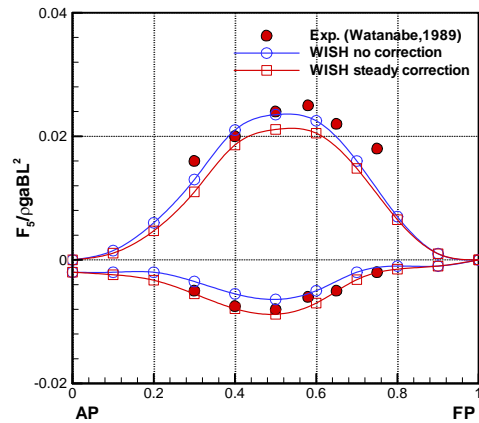
Fig.8 Nonlinear sagging and hogging moments along S715 hull: Hs=L/21, T_0=11.1s, ITTC spectrum, F_n=0.25 , head sea

References

King, B.W., Beck, R.F., Magee, A.R., 1988, "Seakeeping calculations with forward speed using time domain analysis", Proc. of the 17th Symposium on Naval Hydrodynamics, Hague, Netherlands.

Lin, W.M. and Yue, D.K., 1990, "Numerical solutions for large-amplitude ship motions in time domain," Proceedings of the 18th Symposium of Naval Hydrodynamics.

Mantzaris, D. A., 1998, A Rankine panel method as a tool for the hydrodynamic design of complex marine vehicles, PhD Thesis, MIT.

Nakos, D. E., Kring D. C., and Sclavounos, P. D., 1993, "Rankine panel methods for transient free surface flows," Proceedings of the 6th International Conference on Numerical Ship Hydrodynamics.

WISH JIP Phase 1, 2007, Project Report, Seoul National University